Description of terminal substitutional solid solutions using the sublattice model

Jean-Marc Joubert, Jean-Claude Crivello

Description of terminal substitutional solid solutions using the sublattice model

Jean-Marc Joubert, Jean-Claude Crivello

ICMPE, UPEC-CNRS, 2 rue Henri Dunant, 94320, Thiais, France.

e-mail address of corresponding author: joubert@icmpe.cnrs.fr

Keywords: solid solution, sublattice model, DFT calculations, site occupancies, Rietveld method, manganese

Abstract

The case of the substitutional solid solutions based on elements possessing several crystallographic sites is discussed. It is concluded that, at least in some cases, especially when the solution domain is large and when strong differences of site occupancies are observed between the different sites, the sublattice model should be used as it is the case for interstitial solid solutions or non-stoichiometric intermetallic compounds. Results of experimental site occupancies are presented and compared with these obtained from the DFT calculations from which the configurational entropy can be calculated. Comparison of the enthalpy and entropy of the solid solutions is made with the available thermodynamic assessments. The β-U phase in U–Pu system is addressed but the most important cases are α-Mn and β-Mn solid solutions in different systems such as Mn–Re, Fe–Mn, Al–Mn and Al–Fe–Mn. These phases are particularly detailed and conclusions are given relative to their thermodynamic modeling emphasizing the need to use the sublattice model.

1. Introduction

Most elements crystallize in a simple structure possessing a single crystallographic site like it is the case for the most common face-centered cubic (*fcc*), body-centered cubic (*bcc*) and hexagonal close-packed (*hcp*) structures. Terminal substitutional solid solutions based on these elements should be described thermodynamically using a simple substitutional model. However, several elements crystallize in more complex crystal structures involving more than one crystallographic sites. The thermodynamical treatment of the substitutional solid solutions based on these elements (here by substitution we mean that the mechanism is atom replacement, neither vacancy nor interstitial) is systematically made also using the simple substitutional solution model. It will be shown that this is sometimes wrong, because of different site occupancies. It is suggested that the sublattice model should be used which has never been done up to now. Several systems are considered as case studies such as the binaries Pu–U, Mn–Re, Al–Mn, Fe–Mn.

2. Review of the crystal structure of the pure elements

Most metallic elements crystallize in one of the *fcc* (Strukturbericht *A*1), *bcc* (*A*2) or *hcp* (*A*3) crystal structures characterized by the occupation of a single Wyckoff position in the space groups $Fm\bar{3}m$, $Im\bar{3}m$ or $P6_3/mmc$, respectively. Other elements crystallize with specific crystal structures but also with a single site: diamond (*A*4), β-Sn (*A*5), In (*A*6), γ-Se (*A*8)... Specific elements crystallize however in more complex crystal structures that involve more than one crystallographic site and different coordination numbers (CN). Table 1 reports a list of these elements with corresponding crystal structures. Several of these crystal structures are metastable but have indeed been observed in specific conditions (β-Ta with the structure of the σ phase as thin films [1-4], the ω phase in Ti or Ti alloys in certain cooling conditions).

Several elements have crystal structures found only for pure elements (Nd type double *hcp* –*A*3'– for many rare earths at low temperature, β-Mn type –*A*13– for β-Mn). Several other structures correspond to the structure of known intermetallic compounds (the σ phase for β-U, the χ phase –*A*12– for α-Mn). This gives rise to the name of 'single element' or 'self' intermetallic compound attributed to the α and β forms of Mn [5, 6].

In few systems, these elements may form quite extended solid solutions. This is the case for example for β-U in Pu–U system, α-Mn in Fe–Mn and Mn–Re system, β-Mn in Al–Mn and Fe–Mn systems. In the available thermodynamic assessments, they have nonetheless always been treated as simple disordered solid solutions as if they had a single crystallographic site though the crystal structure would suggest a treatment similar to that used for the ordered intermetallic compounds *i.e.* with the use of the Compound Energy Formalism. This is all the more important since the site occupancies of substitutional atoms may be very different on the different sites. In certain systems, a strong tendency to order may be shown. The treatment as a disordered solid solution is no longer appropriate for the modeling and may cause wrong estimation of both the enthalpy and the configurational entropy.

3. Thermodynamical treatment

3.1 Substitutional solutions

Substitutional solid solutions based on elements with *bcc*, *fcc* and *hcp* crystal structures or with any crystal structure involving a single crystallographic site should evidently be treated with the simple solution model (see e.g. [7]).

The Gibbs energy is the sum of a reference term, composition average between the Gibbs energies of the elements in the same structure, an ideal term, calculated from the disordered configurational entropy, and an excess term used to describe the non-ideal enthalpic and entropic interactions in the solution. The excess enthalpy and entropy may be composition dependent but are very rarely temperature dependent.

Let's examine, as an example, the case of the double *hcp* phase (Nd type, *A*3') in Ce–Nd system. At low temperature both elements crystallize in this structure having two distinct crystallographic sites of equal multiplicities 2*a* and 2*c*. They form a continuous solid solution [8]. It is not known if, going from pure Ce to pure Nd by a substitution mechanism, there will be a homogeneous replacement of Ce by Nd on the two sites, or, on the contrary, if it will proceed sequentially by the substitution on

one site then on the other site yielding (at low temperature) an ordered configuration at the equiatomic composition. It is evident that the thermodynamic behavior will be strongly different at this composition between a solid solution with therefore a maximum mixing entropy and an ordered phase with no mixing entropy at all.

Indeed, the thermodynamical treatment as a disordered solid solution may be as wrong as treating an interstitial solid solution like a substitutional one or as treating an ordered intermetallic compound with a homogeneity domain as if it was a single-site solid solution.

3.2 DFT calculations

The formation enthalpy of end-members, generated by the distribution of elements in all available non-equivalent sites of a phase, was calculated by first principles study within the DFT scheme. Calculations were carried out by using the Projector-Augmented Wave (PAW) method performed with the VASP package [9-11]. The Generalized Gradient Approximation (GGA) was used for the exchange and correlation energy with the Perdew-Burke-Ernzerhof functional [12] without the additional Hubbard term for U and Pu element treatment. Calculations implying Fe and Mn have been performed using spin polarization. A plane wave of 600 eV was used for calculations for all the completely relaxed crystal structures. Additional computational details such as accuracy could be found in previous works (e.g. [13]). All the controls have been handled using the ZenGen code [14] (generation of input files, job monitoring, extraction of results).

3.3 Model to compute site occupancies

The thermodynamic properties and site occupancies can be calculated from the DFT calculations of all the configurations obtained by distributing the elements on the different crystal sites and the Compound Energy Formalism [15] without adding any interaction term and using the only ideal configurational entropy on each site (so-called Bragg-Williams approximation). The method is well described in Refs. [16-18].

4. Pu–U system

The β form of uranium has the same structure as the σ phase intermetallic compound (*D8b*, CrFe-type), frequent in many transition metal binary systems. This is a rather complex Frank-Kasper phase involving the presence of 5 different sites. The ordering mechanism in binary (*A*–*B*) systems is well known [19]. The phase has been shown to order around A_2B composition but possesses a strong ability for non-stoichiometry revealed by the presence of very large homogeneity domains. It is accommodated by a large and complex substitutional mechanism likely to occur on each site of the crystal structure.

β-U extends in only few binary systems. Though this is conceptually possible, in a ternary *A*–*B*–U system in which *A*–*B* forms an intermetallic σ phase, it has never been reported to extend enough to observe a continuous phase field between β-U and σ. The binary system in which β-U extends most is

probably Pu–U (27 at.%). Unfortunately, no experimental site occupancy data is available for any of the binary β-U solid solutions. This is due to the technical difficulty to handle uranium, the absence of X-ray contrast between this and other elements with which it forms extended solid solutions (Pu, for example, has only two electron difference), the technical impossibility to perform neutron diffraction on these samples, and also probably to the lack of interest.

We have conducted DFT calculations of the 32 binary configurations generated by the ordered distribution of Pu and U among the 5 different sites of the crystal structure. Calculations were conducted without empirical Hubbard correction. This is justified by the fact that Hubbard correction, necessary to treat localized electrons of actinide elements, is particularly necessary in the case of empty states (gap) close to the Fermi level which is not the case in the Pu–U metallic system. Additionally, no experimental parameter exists in the whole composition range to be fitted in order to adjust the *U* coulomb term. In our case, the electronic structure is probably not very reliable but we are pretty confident in the enthalpies of formation obtained by total energy differences where GGA inaccuracies cancel out. The results are shown in Fig. 1.

Fortunately, a thermodynamic assessment of this system is available [20]. In this work, the β-U phase has, as usual, been treated as a substitutional solid solution. Energetically, our DFT results of the enthalpies of formation of ordered compounds compare well with the assessed mixing enthalpy for the disordered substitutional solid solution (Fig. 1). This shows that, despite the difficulties and approximations, our calculations are reliable.

From these calculations, the site occupancies can be computed using the compound energy formalism. They are presented in Fig. 2 at 1000 K, the temperature at which the solution extends most. According to the ground state of Fig. 1, the distribution of atoms is ordered with a progressive and sequential occupancy of different sites when changing the composition from pure Pu to pure U. One should take note that the sequential order is not the one usually observed for the intermetallic σ phase. From these results, the configurational entropy can be calculated as a function of composition and it is shown in Fig. 3 in comparison with the ideal configurational entropy used in the model of Perron *et al.* [20] and the assessed mixing entropy. As for the enthalpies, the use of an interaction parameter allows to correct the deficiency of the model and reproduce artificially the configurational entropy by using an excess term.

5. α-Mn *A*12 solid solutions

α-Mn has the same structure as the Frank-Kasper intermetallic χ phase. This phase appears in a large number of intermetallic systems. A review of the crystal structure property of this phase and recommendations for its modeling are given in Ref. [21]. It contains four crystallographic sites 2*a*, 8*c*, 24g_1, 24g_2 in the space group *I*-43*m*.

Ref. [21] also treats the case of the solid solutions based on α-Mn. It is shown that the solid solution may extend quite extensively in several systems (with a maximum of 60 at.% in the case of Mn–Re system), that the solute orders quite significantly (it replaces Mn in given, specific crystallographic sites) and that, depending on the element, the nature of the sites occupied may be different. Cr, Mo,

Re, Ti and V replace Mn on sites 2*a* and 8*c* and then 24g_1, while Fe, Ni, Ru replace Mn preferentially on 24g_2, mainly for geometrical reasons.

Fig. 4 shows the results of the DFT calculation of all the ordered configurations in Mn–Re system. From this calculation, the site fractions may be calculated in the compound energy formalism and may be compared with the experimental site occupancy data [21, 22] as shown in Fig. 5. The qualitative agreement is very good though the quantitative agreement is only relative. Nevertheless, calculations of the entropy of mixing in three different scenarios (from DFT calculation and the compound energy formalism, from the experimental site occupancies, from the ideal entropy obtained when modeling the phase as a simple solid solution, Fig. 6) shows the inability to describe correctly the entropy with the latter model. One could argue that this could be compensated by an excess entropy in the modeling as this was observed in Pu–U system in Section 4. But this can be at only one temperature since the excess entropy is not temperature dependent, whereas the site occupancies change as a function of temperature. In Pu–U system, this was acceptable because the temperature range of existence of β-U phase is petty limited which is no longer the case in Mn–Re system that has to be described from 300 to 1300 K.

6. β-Mn

Another allotropic structure of Mn is β-Mn. It has a unique crystal structure found only for this element. It is described in space group $P4_132$ with occupied crystallographic sites 8*c* (CN12) and 12*d* (CN14). The coordination is very similar to that found in intermetallic compounds and the structure itself has been classified as a Frank-Kasper phase. It has extended (over 10 at.%) solid solution domains in binary systems with Al, Fe, Ga, Ge, In, Ni, Ru, Si, Sn, V and reaching 50 at.% in the case of Co and Zn (see Fig. 7).

DFT calculations have been carried out in order to determine the level of ordering of the solute in the two systems Al–Mn and Fe–Mn in which the solubility is 40 at.% and 30 at.%, respectively.

For Fe–Mn system, the calculation of the four ordered configurations generated by the distribution of the two elements on the two crystallographic sites is presented in Fig. 8. The resulting calculation of the site occupancies is in Fig. 9. A comparison of the energies is made with the thermodynamic assessment by Djurovic *et al.* [23] who treated the β-Mn phase as a simple solid solution showing a reasonable agreement with our DFT calculations. The ordering between the two different sites is not very strong due to the relatively weak formation energy of the more stable intermediate end-member. In this case, the approximation by a substitutional solid solution model seems quite reasonable in terms of energetics, site occupancies and configurational entropy.

The same type of calculation has been performed for the Al–Mn system. In this system, the situation is completely different. The system is much more exothermic (Fig. 10). The ordered configuration Mn:Al has a formation energy of around -23 kJ/mol (in extremely good agreement with the thermodynamic assessment by Du *et al.* [24]) and a large difference is observed with the formation energy of the anti-structure. This results in a very ordered atomic distribution as shown in Fig. 11. Al has a very strong tendency to occupy the CN14 site with higher coordination, as a large atom is expected to have. The resulting configurational entropy calculated at 973 K compared with the ideal

entropy of single site solid solution shows the inability of this model to describe properly the thermodynamic properties of this phase especially at high Al concentrations (Fig. 12).

The situation is even worse in the ternary Al–Fe–Mn system because the β-Mn phase extends even more in the ternary system than in the two binaries (see Fig. 13). Compositions with Mn content as low as 30 at.% can be reached revealing that the phase should truly be described over an extremely wide composition domain not limited to the Mn rich compositions.

Ternary site occupancy calculations have also been calculated for this system and are shown in Fig. 14 along the line drawn on the phase diagram of Fig. 13 from pure Mn to AlFe. Again, this shows the strong ordering of Al atoms in the structure as expected from the binary system.

7. Discussion

7.1. Ordering

It should be noted that the ordering observed in this type of solution is rather different from the ordering observed in classical solid solutions (like, for example, in Au–Cu system the ordering of *fcc* into $L1_0$ or $L1_2$ structures). In this case the different Wyckoff positions originate from the ordering at special binary compositions (1:1 for $L1_0$, 1:3 or 3:1 for $L1_2$) by a splitting of an original single position. There is a (first or second) order-disorder transition and order does not exist in diluted solid solution close to pure elements. Our case is very different since the ordering takes place because of the original presence of different Wyckoff positions already in the pure metal. So that ordering occurs in the very diluted solid solutions. There is no order-disorder transition.

The kind of solid solutions addressed in the present work, based on elements whose crystal structure possesses more than one non-equivalent crystallographic site, must be distinguished from the classical solid solutions in which a single crystallographic site is involved like *fcc*, *bcc* or *hcp*. As discussed above, they have also to be distinguished from the ordered solid solutions based on these structures.

They share common points with the interstitial solid solutions since the stability domain starts from the pure element and several crystal sites are involved. They also show similarity with non-stoichiometric intermetallic compounds in which the non-stoichiometry is accommodated by a substitution mechanism on different sites. In this regard, they deserve a special thermodynamic treatment.

7.2. Thermodynamical treatment

We have shown that this phenomenon may have important consequences. This is because the solution domain has not always an insignificant extension. On the contrary, it may be very large reaching 50 at.% for both α and β-Mn in some systems. We have also seen at least one example where the concentration of the 'solvent' may reach only 30 at.% (Mn in the ternary Al–Fe–Mn system). This is important also because the extent of ordering may be significant. We have shown that it was not the case in the β-Mn solution domain of Fe–Mn system, but it is certainly the case in

the binary Al–Mn system. Finally, if the significance may be only relative for β-U solid solutions, it is certainly important for all Mn-based systems given the technological importance of these systems. An inaccurate description of α and β-Mn solid solutions in systems such as Mn–Fe or Mn–Co in databases may cause problems in the extrapolation done for multi-component systems like steels or superalloys. For example, in a study of high-entropy alloys, Bracq *et al.* [25] showed an alloy (alloy G in their paper) predicted by the TCHEA database to be *fcc* while it is shown experimentally to be a single phase β-Mn alloy. This shows the underestimation of the stability of β-Mn in the commercial database. The inadequate model may not be the only explanation for the discrepancy but it is probably part of it.

As we exposed, the classical solid solution model always used to describe these solutions is not appropriate. To a certain extent, the convex hull at 0 K marked by the existence of stable intermediate configurations can be satisfactorily approximated using excess terms (see eg. Fig. 1 or 10). However, the entropy can certainly not be reproduced. The ideal entropy of a classical disordered solid solution can evidently not take into account the ordering at particular compositions. Even a correction using an excess entropy should not be able to compensate the difference. If it does to certain extent at a given temperature, it can probably not at a different temperature because in an ordered model the mixing entropy changes as a function of temperature as the site fractions do while the excess entropy would be constant unless a very complicated unmanageable model is used. This is the limitation of using a solid solution model.

It is therefore suggested to use systematically the Compound Energy Formalism for the modeling of terminal solid solutions based on an element having more than a single crystallographic site. In the case of α-Mn, this implies using at least 3 sublattices (see the complete description of the modeling of the χ phase in Ref. [21]). For the β-Mn, a two sublattice model should be used. Parameters corresponding to the different end-members should be determined. For this, systematic DFT calculations are advised not only for unary but also for binary end-members. Furthermore, there is a need for experimental site occupancy measurements in particular for the β-Mn phase.

8. Conclusion

Using a simple substitutional model for the description of terminal solid solutions based on elements possessing different sites may be as wrong as using this type of model for ordered phases such as non-stoichiometric compounds or interstitial solid solutions. By the time one is looking for more accurate descriptions and models within the Calphad approach (description down to 0 K [26, 27], use of models fully compatible with the crystal structure of compounds (see eg. [28, 29])), it is strongly advised to take care of this problem and to use eventually, for solid solutions with several crystallographic sites a model fully compatible with the crystal structure dividing the structure into different sublattices.

Acknowledgments

Aurélien Perron, Weisen Zheng and Xiao-Gang Lu are acknowledged for sharing their TDB files and for fruitful discussions. DFT calculations were performed using HPC resources from GENCI-CINES (Grant 2019-96175).

Data availability

Data will be made available on request.

Table 1: pure element crystal structures containing more than a single lattice site (source: [30]). The list is not exhaustive, exotic crystal structures and elements have been removed. Elements adopting the structure in their stable form are indicated in bold.

Prototype	Strukturbericht	Pearson's symbol	Number of sites	Elements
Nd	*A*3'	*hP*4	2	Ag, Am, Bk, **Ce**, Cf, Cm, Dy, Er, Gd, **La**, **Nd**, Pm, **Pr**, Sm, Tb, Tm
α-Np	A_c	*oP*8	2	**Np**
β-Np	A_d	*tP*4	2	**Np**, Sc
Sm		*hR*9	2	Dy, Er, Gd, Ho, Li, Na, **Sm**, Tb, Tm
Pu		*mP*16	8	**Pu**
Pu		*mS*34	7	**Pu**
CrFe (σ phase)	A_b, $D8_b$	*tP*30	5	Ta,**U**
α-Mn (χ phase)	*A*12	*cI*58	4	**Mn**
β-Mn	*A*13	*cP*20	2	Co, **Mn**, Re
Ti (ω phase)		*hP*3	2	Ti, Zr

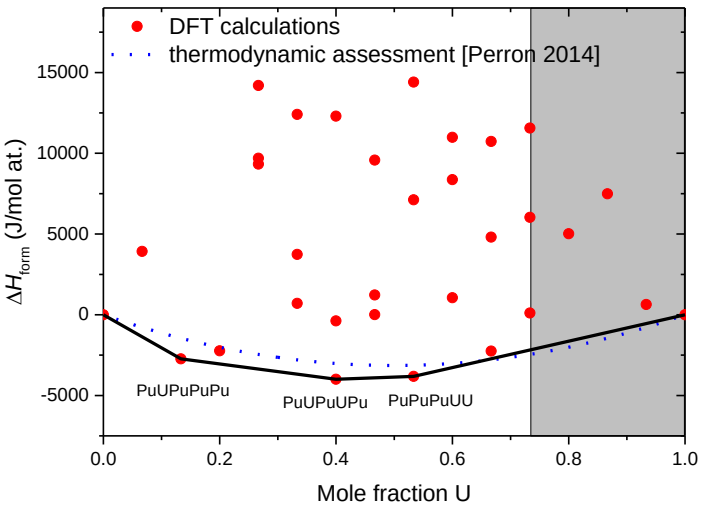

Figure 1: DFT calculations of the 32 end-members of the σ phase in Pu–U system (references σ-Pu and σ-U), ground-state and comparison with the thermodynamic assessment of Perron *et al.* [20]. The experimental stability range of the phase is shaded in grey.

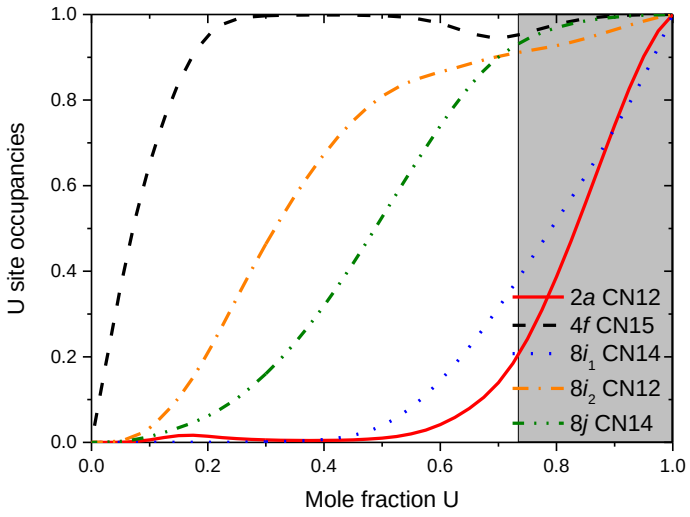

Figure 2: computed site occupancies at 1000 K in the σ phase of Pu–U system. The experimental stability range of the phase is shaded in grey.

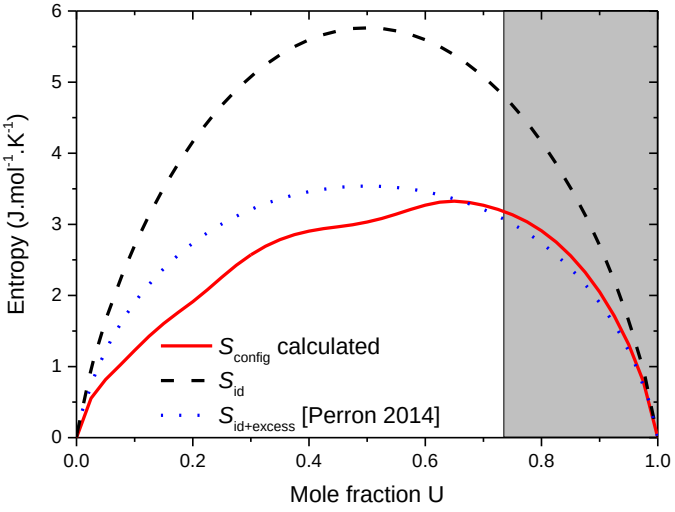

Figure 3: configurational entropy from the DFT-calculated site occupancies at 1000 K compared with the ideal configurational entropy in a solid solution and the entropy from the thermodynamic assessment of Perron *et al.* [20]. The experimental stability range of the phase is shaded in grey.

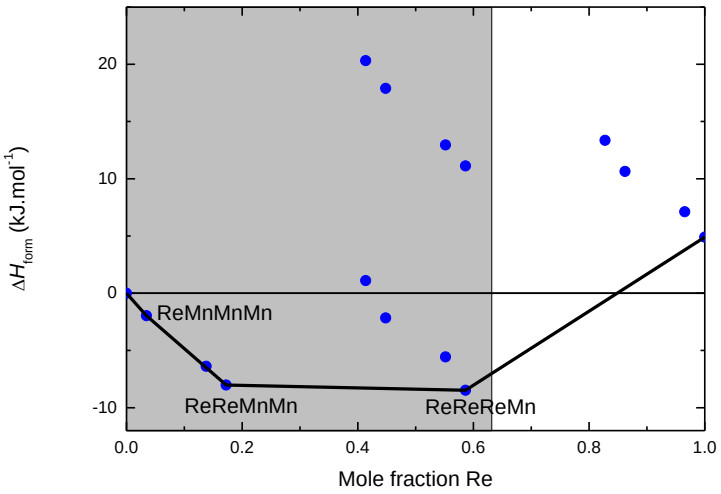

Figure 4: DFT calculations of the 16 end-members of the α-Mn phase in Mn–Re system (references α-Mn and *hcp* Re) and ground state. The experimental stability range of the phase is shaded in grey.

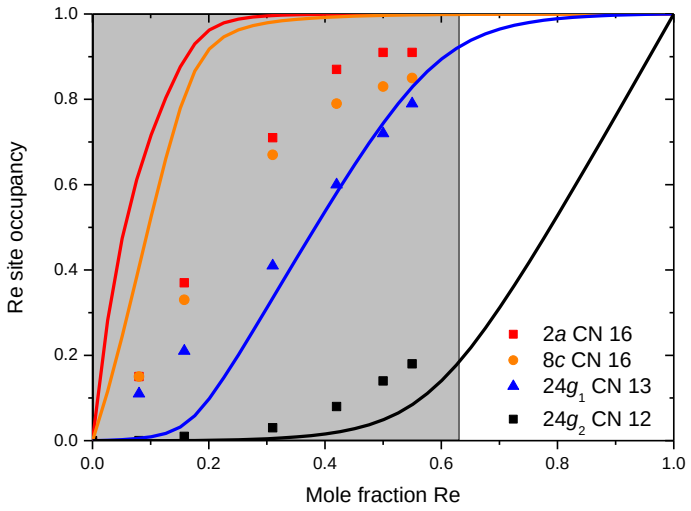

Figure 5: experimental and DFT-calculated site occupancies at 1123 K in the α-Mn phase of Mn–Re system. The experimental stability range of the phase is shaded in grey.

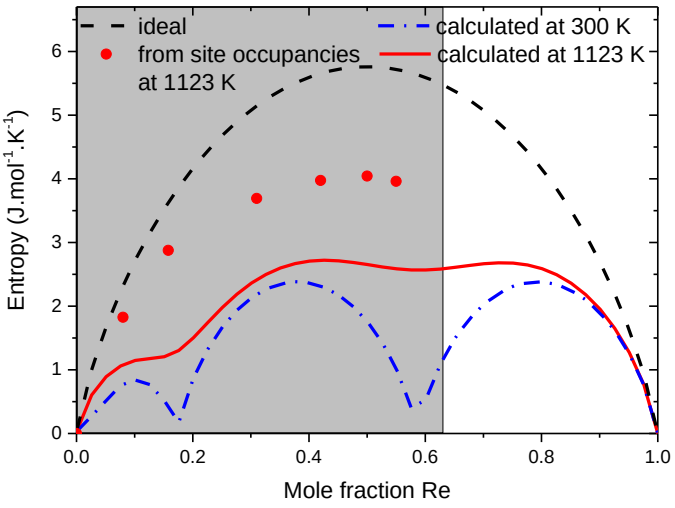

Figure 6: configurational entropy from the experimental and DFT-calculated site occupancies compared with the ideal configurational entropy in a solid solution. The experimental stability range of the phase is shaded in grey.

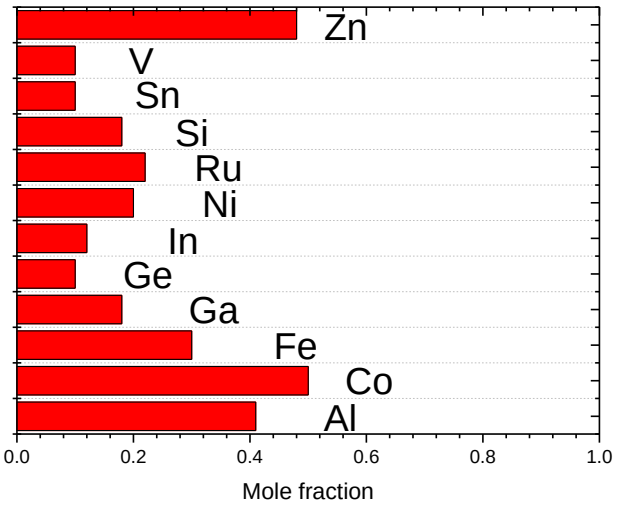

Figure 7: solubility in β-Mn phase in different Mn-*X* systems.

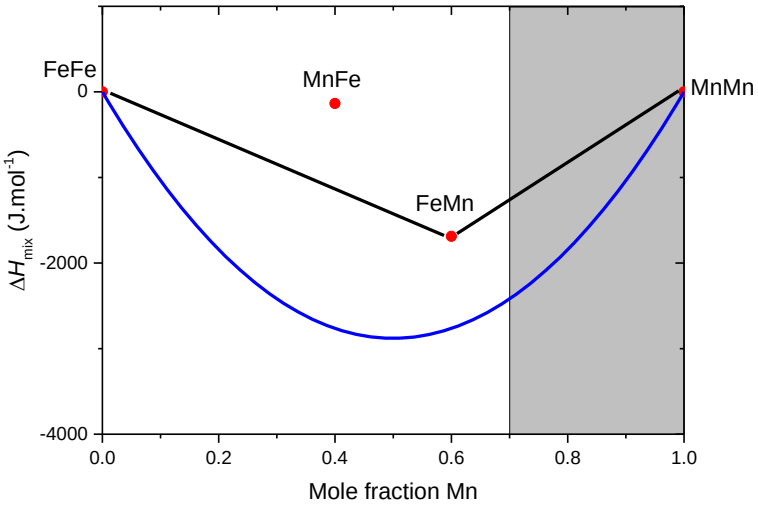

Figure 8: DFT calculations of the 4 end-members of the β-Mn phase in Fe–Mn system (references β-Mn and Fe in β-Mn structure), ground state and comparison with the thermodynamic assessment of Djurovic *et al.* [23]. The experimental stability range of the phase is shaded in grey.

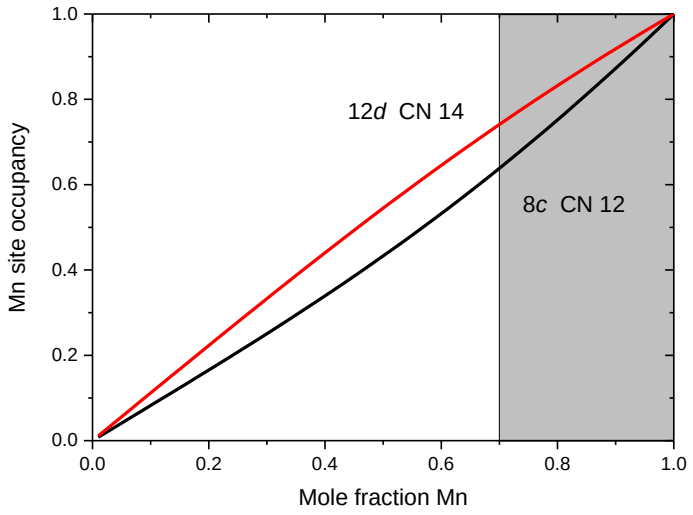

Figure 9: DFT-calculated site occupancies at 973 K in the β-Mn phase of the Fe–Mn system. The experimental stability range of the phase is shaded in grey.

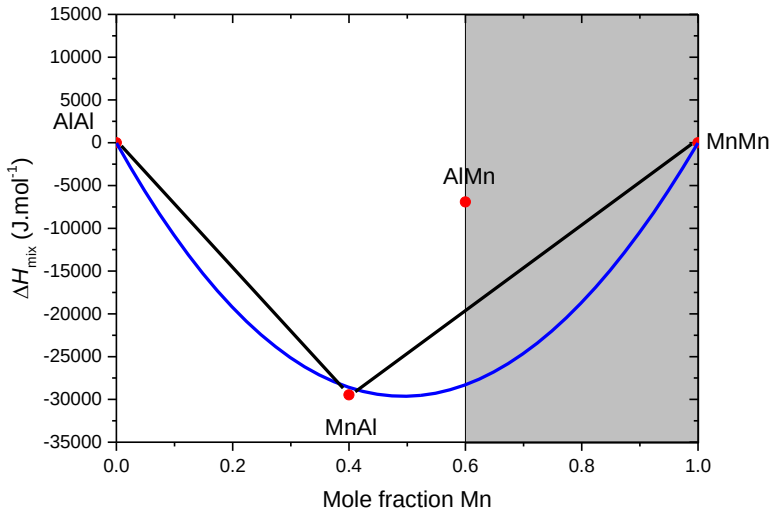

Figure 10: DFT calculations of the 4 end-members of the β-Mn phase in Al–Mn system (references β-Mn and Al in β-Mn structure), ground state and comparison with the thermodynamic assessment of Du *et al.* [24]. The experimental stability range of the phase is shaded in grey.

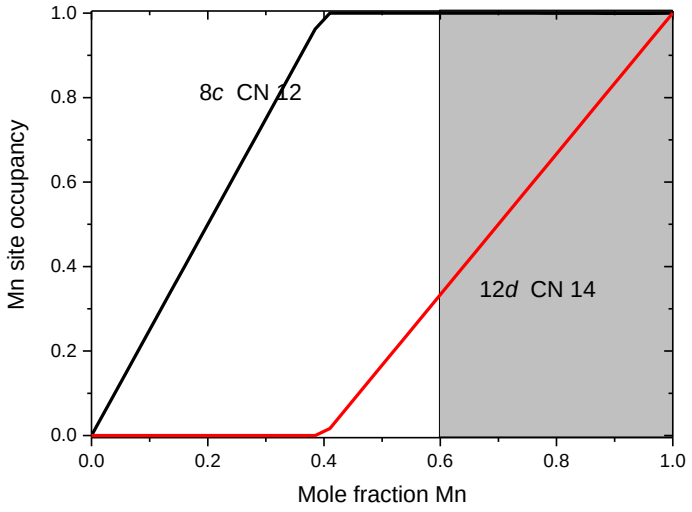

Figure 11: DFT-calculated site occupancies at 973 K in the β-Mn phase of the Al–Mn system. The experimental stability range of the phase is shaded in grey.

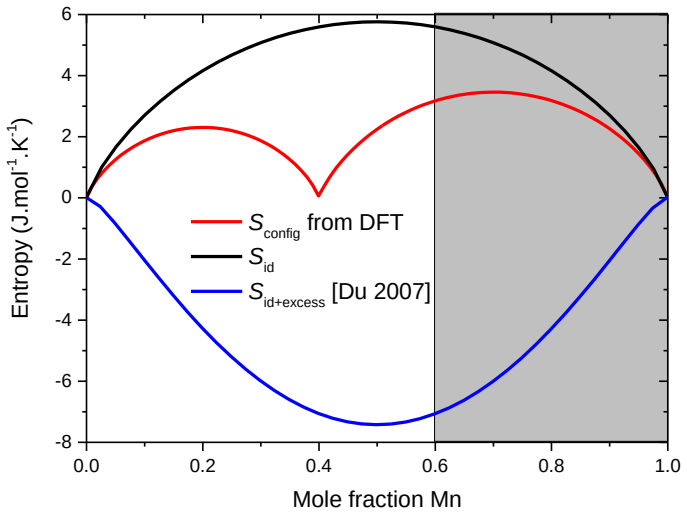

Figure 12: configurational entropy from the DFT-calculated site occupancies at 973 K compared with the ideal configurational entropy in a solid solution and the entropy from the thermodynamic assessment of Du *et al.* [24]. The experimental stability range of the phase is shaded in grey.

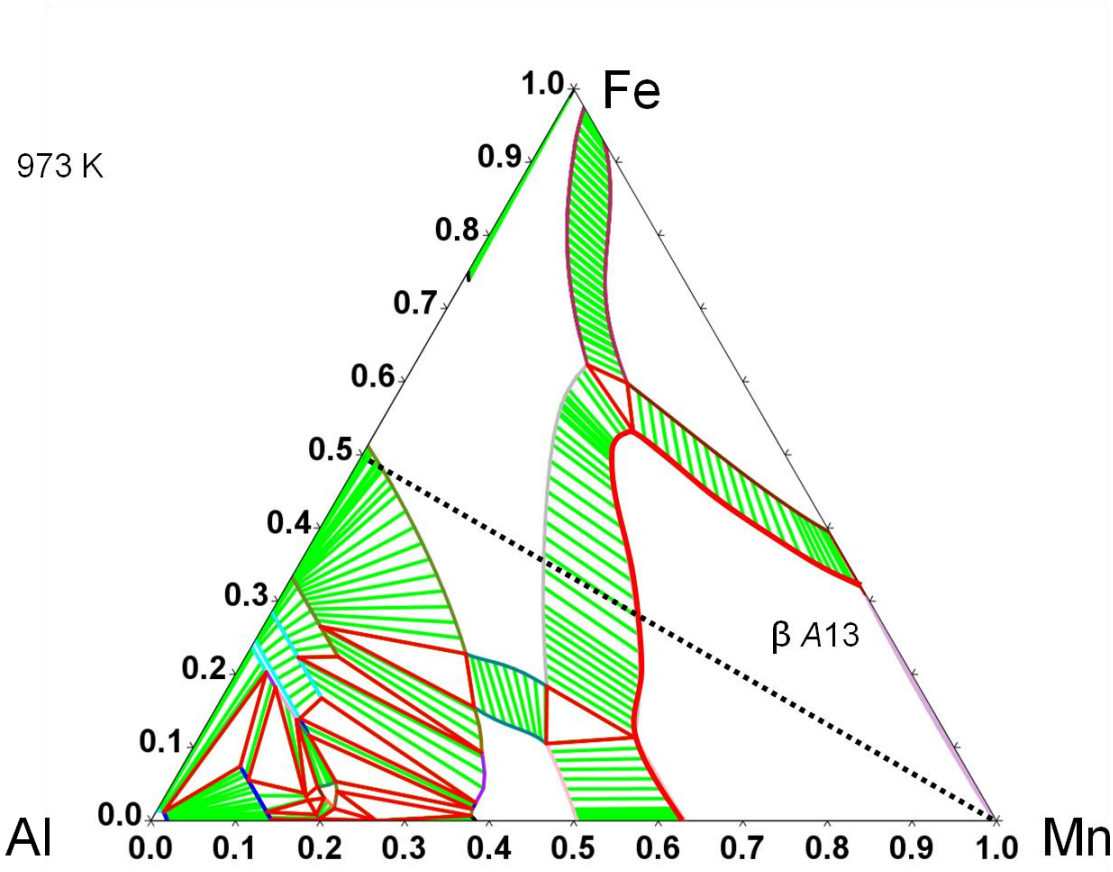

Figure 13: Al–Fe–Mn isothermal section at 973 K from the thermodynamical assessment of Zheng *et al.* [31].

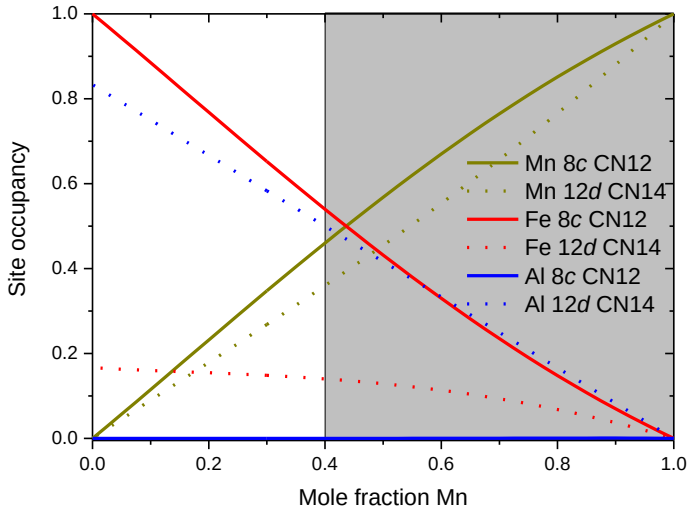

Figure 14: computed ternary site occupancies from the DFT calculations in the β phase of the Al–Fe–Mn system along the dotted line drawn in Fig. 13 (AlFe to Mn). The experimental stability range of the phase is shaded in grey.

References:

[1] A. Arakcheeva, G. Chapuis, V. Grinevitch, The self-hosting structure of β-Ta, Acta Crystallogr. B58 (2002) 1-7. https://doi.org/10.1107/S0108768101017918.

[2] A. Arakcheeva, G. Chapuis, H. Birkedal, P. Pattison, V. Grinevitch, The commensurate composite σ-structure of β-tantalum, Acta Crystallogr. B59 (2003) 324-336. https://doi.org/10.1107/S0108768103009005.

[3] A. Jiang, A. Yohannan, N.O. Nnolim, T.A. Tyson, L. Axe, S.L. Lee, P. Cote, Investigation of the structure of β-tantalum, Thin Solid Films 437 (2003) 116-122. https://doi.org/10.1016/S0040-6090(03)00702-8.

[4] P.T. Moseley, C.J. Seabrook, The crystal structure of β-tantalum, Acta Crystallogr. B29 (1973) 1170-1171. https://doi.org/10.1107/S0567740873004140.

[5] A.J. Bradley, J. Thewlis, The crystal structure of α-manganese, Proc. R. Soc. (London) A115 (1927) 459-471. https://doi.org/10.1098/rspa.1927.0103.

[6] A.C. Lawson, A.C. Larson, M.C. Aronson, S. Johnson, Z. Fisk, P.C. Canfield, J.D. Thompson, R.B. Von Dreele, Magnetic and crystallographic order in α-manganese, J. Appl. Phys. 76 (10) (1994) 7049-7051. https://doi.org/10.1063/1.358024.

[7] H.L. Lukas, S.G. Fries, B. Sundman. Computational Thermodynamics, the Calphad Method, Cambridge, New York, Melbourne, Madrid, Cape Town, Singapore, São Paulo: Cambridge University Press, 2007.

[8] T.B. Massalski. Binary alloys phase diagrams, second ed., ASM International, Materials Park, Ohio, 1990.

[9] G. Kresse, J. Hafner, Ab initio molecular dynamics for open-shell transition metals, Phys. Rev., B 48 (1993) 13115. https://doi.org/10.1103/PhysRevB.48.13115.

[10] G. Kresse, J. Furthmüller, Efficient iterative schemes for ab initio total-energy calculations using a plane-wave basis set, Phys. Rev., B 54 (1996) 11169-11186. https://doi.org/10.1103/PhysRevB.54.11169.

[11] G. Kresse, D. Joubert, From ultrasoft pseudopotentials to the projector augmented-wave method, Phys. Rev., B 59 (3) (1999) 1758-1775. https://doi.org/10.1103/PhysRevB.59.1758.

[12] J.P. Perdew, K. Burke, M. Ernzerhof, Generalized gradient approximation made simple, Phys. Rev. Lett. 77 (18) (1996) 3865-3868. https://doi.org/10.1103/PhysRevLett.77.3865.

[13] J.-C. Crivello, M. Palumbo, T. Abe, J.-M. Joubert, Ab initio ternary σ-phase diagram: the Cr–Mo–Re system, Calphad: Comput. Coupling Phase Diagrams Thermochem. 34 (2010) 487-494. https://doi.org/10.1016/j.calphad.2010.09.002.

[14] J.-C. Crivello, R. Souques, N. Bourgeois, A. Breidi, J.-M. Joubert, ZenGen: a tool to generate ordered configurations for systematic DFT calculations: example of the Cr-Mo-Ni-Re system, Calphad: Comput. Coupling Phase Diagrams Thermochem. 51 (2015) 233-240. https://doi.org/10.1016/j.calphad.2015.09.005.

[15] B. Sundman, J. Ågren, A regular solution model for phases with several components and sublattices, suitable for computer applications, J. Phys. Chem. Solids 42 (1981) 297-301. https://doi.org/10.1016/0022-3697(81)90144-X.

[16] S.G. Fries, B. Sundman, Using Re-W sigma phase first-principles results in the Bragg-Williams approximation, Phys. Rev., B 66 (2002) 012203. https://doi.org/10.1103/PhysRevB.66.012203.
[17] N. Dupin, S.G. Fries, J.-M. Joubert, B. Sundman, M. Sluiter, Y. Kawazoe, A. Pasturel, Using Nb-Ni μ phase first principles results in the Bragg-Williams approximation to calculate finite temperature thermodynamic properties, Philos. Mag. 86 (12) (2006) 1631-1641. https://doi.org/10.1080/14786430500437488.
[18] J.-M. Joubert, J.-C. Crivello, M. Andasmas, P. Joubert, Phase stability in the ternary Re-W-Zr system, Acta Mater. 70 (2014) 56-65. https://doi.org/10.1016/j.actamat.2014.02.010.
[19] J.-M. Joubert, Crystal chemistry and Calphad modelling of the σ phase, Prog. Mater. Sci. 53 (2008) 528-583. https://doi.org/10.1016/j.pmatsci.2007.04.001.
[20] A. Perron, P.E.A. Turchi, A. Landa, P. Söderlind, B. Ravat, B. Oudot, F. Delaunay, M. Kurata, Thermodynamic re-assessment of the Pu-U system and its application to the ternary Pu-U-Ga system, J. Nucl. Mater. 454 (2014) 81-95. https://doi.org/10.1016/j.jnucmat.2014.07.051.
[21] J.-M. Joubert, M. Phejar, The crystal chemistry of the χ phase, Prog. Mater. Sci. 54 (7) (2009) 945-980. https://doi.org/10.1016/j.pmatsci.2009.04.002.
[22] Y. Graz, J.-M. Fiorani, N. David, J.-M. Joubert, M. Vilasi, Experimental study of the Mn-Re system, J. Alloys Compd. 575 (2013) 344-349. http://dx.doi.org/10.1016/j.jallcom.2013.05.154.
[23] D. Djurovic, B. Hallstedt, J. von Appen, R. Dronskowski, Thermodynamic assessment of the Fe-Mn-C system, Calphad: Comput. Coupling Phase Diagrams Thermochem. 35 (2011) 479-491. https://doi.org/10.1016/j.calphad.2011.08.002.
[24] Y. Du, J. Wang, J. Zhao, J.C. Schuster, F. Weitzer, R. Schmid-Fetzer, M. Ohno, H. Xu, Z.-K. Liu, S. Shang, W. Zhang, Reassessment of the Al-Mn system and a thermodynamic description of the Al-Mg-Mn system, Int. J. Mater. Res. 98 (9) (2007) 855-871. https://doi.org/10.3139/146.101547.
[25] G. Bracq, M. Laurent-Brocq, L. Perrière, R. Pirès, J.-M. Joubert, I. Guillot, The fcc solid solution stability in the Co-Cr-Fe-Mn-Ni multi-component system, Acta Mater. 128 (2017) 327-336. https://doi.org/10.1016/j.actamat.2017.02.017.
[26] Y. Jiang, S. Zomorodpoosh, I. Roslyakova, L. Zhang, Thermodynamic re-assessment of binary Cr-Nb system down to 0 K, Calphad 62 (2018) 109-118. https://doi.org/10.1016/j.calphad.2018.06.001.
[27] S. Bigdeli, Q. Chen, M. Selleby, A new description of pure C in developing the third generation of Calphad databases, J. Phase Equilibr. Diffus. 39 (2018) 832-840. https://doi.org/10.1007/s11669-018-0679-3.
[28] R. Mathieu, N. Dupin, J.-C. Crivello, K. Yaqoob, A. Breidi, J.-M. Fiorani, N. David, J.-M. Joubert, CALPHAD description of the Mo-Re system focused on the sigma phase modeling, Calphad: Comput. Coupling Phase Diagrams Thermochem. 43 (2013) 18-31. https://doi.org/10.1016/j.calphad.2013.08.002.
[29] B. Sundman, Q. Chen, Y. Du, A review of Calphad modeling of ordered phases, J. Phase Equilibr. Diffus. 39 (5) (2018) 678-693. https://doi.org/10.1007/s11669-018-0671-y.
[30] H. Putz, K. Brandenburg. Pearson's Crystal Data: Crystal Structure Database for Inorganic Compounds, version 2.1, ASM International, Materials Park, Ohio, USA and Material Phases Data System, Vitznau, Switzerland, 2017/2018.
[31] W. Zheng, H. Mao, X.-G. Lu, Y. He, L. Li, M. Selleby, J. Ågren, Thermodynamic investigation of the Al-Fe-Mn system over the whole composition and wide temperature ranges, J. Alloys Compd. 742 (2018) 1046-1057. https://doi.org/10.1016/j.jallcom.2018.01.291.